TU/e EINDHOVEN UNIVERSITY OF TECHNOLOGY

Atomic layer deposition of wet-etch resistant silicon nitride using di(sec-butylamino) silane and N2 plasma on planar and 3D substrate topographies

Citation for published version (APA):
Faraz, T., van Drunen, M., Knoops, H. C. M., Mallikarjunan, A., Buchanan, I., Hausmann, D. M., Henri, J., & Kessels, W. M. M. (2017). Atomic layer deposition of wet-etch resistant silicon nitride using di(sec-butylamino) silane and N2 plasma on planar and 3D substrate topographies. *ACS Applied Materials & Interfaces*, *9*(2), 1858-1869. https://doi.org/10.1021/acsami.6b12267

Document license:
TAVERNE

DOI:
10.1021/acsami.6b12267

Document status and date:
Published: 18/01/2017

Document Version:
Publisher's PDF, also known as Version of Record (includes final page, issue and volume numbers)

Please check the document version of this publication:

• A submitted manuscript is the version of the article upon submission and before peer-review. There can be important differences between the submitted version and the official published version of record. People interested in the research are advised to contact the author for the final version of the publication, or visit the DOI to the publisher's website.
• The final author version and the galley proof are versions of the publication after peer review.
• The final published version features the final layout of the paper including the volume, issue and page numbers.

Link to publication

General rights
Copyright and moral rights for the publications made accessible in the public portal are retained by the authors and/or other copyright owners and it is a condition of accessing publications that users recognise and abide by the legal requirements associated with these rights.

• Users may download and print one copy of any publication from the public portal for the purpose of private study or research.
• You may not further distribute the material or use it for any profit-making activity or commercial gain
• You may freely distribute the URL identifying the publication in the public portal.

If the publication is distributed under the terms of Article 25fa of the Dutch Copyright Act, indicated by the "Taverne" license above, please follow below link for the End User Agreement:

www.tue.nl/taverne

Take down policy
If you believe that this document breaches copyright please contact us at:

openaccess@tue.nl

providing details and we will investigate your claim.

Download date: 04. Oct. 2023

ACS APPLIED MATERIALS & INTERFACES

Research Article

www.acsami.org

Atomic Layer Deposition of Wet-Etch Resistant Silicon Nitride Using Di(*sec*-butylamino)silane and N_2 Plasma on Planar and 3D Substrate Topographies

Tahsin Faraz,*[,†,¶] Maarten van Drunen,[†,¶] Harm C. M. Knoops,[†,‡] Anupama Mallikarjunan,[§] Iain Buchanan,[§] Dennis M. Hausmann,[⊥] Jon Henri,[⊥] and Wilhelmus M. M. Kessels*[,†]

[†]Eindhoven University of Technology, P.O. Box 513, 5600 MB Eindhoven, The Netherlands

[‡]Oxford Instruments Plasma Technology, North End, Bristol BS49 4AP, U.K.

[§]Air Products and Chemicals Inc., 1969 Palomar Oaks Way, Carlsbad, California 92011, United States

[⊥]Lam Research Corporation, 11155 Southwest Leveton Drive, Tualatin, Oregon 97062, United States

Supporting Information

ABSTRACT: The advent of three-dimensional (3D) finFET transistors and emergence of novel memory technologies place stringent requirements on the processing of silicon nitride (SiN_x) films used for a variety of applications in device manufacturing. In many cases, a low temperature (<400 °C) deposition process is desired that yields high quality SiN_x films that are etch resistant and also conformal when grown on 3D substrate topographies. In this work, we developed a novel plasma-enhanced atomic layer deposition (PEALD) process for SiN_x using a mono-aminosilane precursor, di(*sec*-butylamino)silane (DSBAS, $SiH_3N(^sBu)_2$), and N_2 plasma. Material properties have been analyzed over a wide stage temperature range (100−500 °C) and compared with those obtained in our previous work for SiN_x deposited using a bis-aminosilane precursor, bis(*tert*-butylamino)silane (BTBAS, $SiH_2(NH^tBu)_2$), and N_2 plasma. Dense films (~3.1 g/cm^3) with low C, O, and H contents at low substrate temperatures (<400 °C) were obtained on planar substrates for this process when compared to other processes reported in the literature. The developed process was also used for depositing SiN_x films on high aspect ratio (4.5:1) 3D trench nanostructures to investigate film conformality and wet-etch resistance (in dilute hydrofluoric acid, HF/H_2O = 1:100) relevant for state-of-the-art device architectures. Film conformality was below the desired levels of >95% and attributed to the combined role played by nitrogen plasma soft saturation, radical species recombination, and ion directionality during SiN_x deposition on 3D substrates. Yet, very low wet-etch rates (WER ≤ 2 nm/min) were observed at the top, sidewall, and bottom trench regions of the most conformal film deposited at low substrate temperature (<400 °C), which confirmed that the process is applicable for depositing high quality SiN_x films on both planar and 3D substrate topographies.

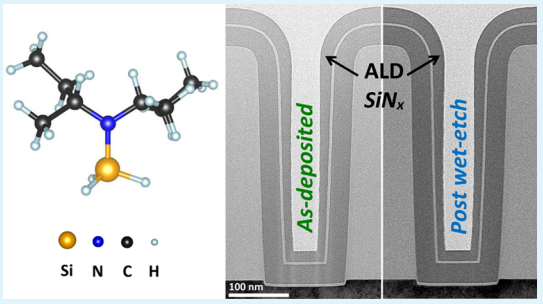

KEYWORDS: *silicon nitride, atomic layer deposition, ALD, plasma ALD, di(sec-butylamino)silane, DSBAS, thin film, wet etch*

INTRODUCTION

Silicon nitride (SiN_x) is a widely used material in both front and back end-of-the-line (FEOL/BEOL) processes of semiconductor device manufacturing.[1,2] It regularly serves as hard masks and etch stop layers in critical processing techniques such as spacer defined patterning[3−5] and self-aligned contacts.[6,7] A key application of SiN_x films is spacers[8−10] for the high-k metal gate (HKMG) stack in both planar FET and state-of-the-art 3D finFET[11−13] architectures in CMOS nanoelectronics. These spacer films serve multiple purposes such as being a barrier against oxygen ingress and dopant out-diffusion while preventing any etch damage during subsequent processing steps.[14,15] They also provide a constant spacing of the source and drain of the transistor, independent of transistor pitch.[8,16] All these require the SiN_x films to be highly conformal and etch resistant in dilute hydrofluoric (HF) acid (HF/H_2O = 1:100).[8,14,15] However, the use of the HKMG stack requires a low temperature (~400 °C) processing environment to prevent interlayer diffusion or interfacial reactions from occurring at elevated temperatures.[17] Processing of SiN_x at even lower temperatures (~250 °C) is required for applications in emerging memory devices, such as encapsulation[18] for magnetic tunnel junctions (MTJ) in MRAMs,[19−21] where metal atom migration at high temperatures can lead to device degradation.[21−24] SiN_x has been traditionally deposited using low-pressure chemical vapor deposition (LPCVD) or plasma-enhanced chemical vapor deposition (PECVD) processes.[25] LPCVD generally yields conformal SiN_x films with low wet-

Received: September 27, 2016
Accepted: December 5, 2016
Published: December 5, 2016

ACS Publications © 2016 American Chemical Society

DOI: 10.1021/acsami.6b12267
ACS Appl. Mater. Interfaces 2017, 9, 1858−1869

Table 1. Overview of SiN_x Material Properties Reported in the Literature for Films Deposited with ALD Using Various Precursors and Coreactants[a]

precursor	coreactant	mass density (g/cm^3)	3D substrate aspect ratio	conformality (side/top ratio in %)	wet-etch rate (nm/min)		ref
					planar surface	3D sidewall surface	
$SiCl_4$, SiH_2Cl_2, Si_2Cl_6, Si_3Cl_8	NH_3, NH_3 plasma, N_2H_4	<2.7[b]	≥2:1[c]	>80[c]	>10[d]	-	15, 31−37
SiH_4	N_2 plasma	2.7	~3.5:1	≤50	-	-	25
$N(SiH_3)_3$	H_2/N_2 plasma	2.8	~2:1	~80	≤1.5	-	14
$N(SiHN(CH_3)_2CH_3)_2Si(CH_3)_3$	N_2 plasma	-	~5.5:1	~73	≤4.55[e]	-	39
$Si(SiH_3)_4$	N_2 plasma	2.21	≥6:1	~50	~3	-	40
$SiH_2(NH^tBu)_2$	N_2 plasma	2.9	-	-	~0.2	-	16
$SiH_3N(^sBu)_2$	N_2 plasma	≤3.1	4.5:1	≤50	0−2	1−6	this work[f]

[a]The selected reports are chosen based on data available for film conformality on 3D substrate topographies and wet-etch resistance (in dilute hydrofluoric acid, HF/H_2O = 1:100) of SiN_x at planar and 3D surfaces when deposited at temperatures ≤400 °C. A "-" indicates data not reported. [b]Data available only for refs 31, 33, and 37. [c]Data available only for refs 15, 36, and 37. [d]Data available only for refs 15 and 36. [e]Wet-etch rate reported using dilute HF solution with HF/H_2O = 1:500. [f]For substrate temperatures <400 °C.

etch rates (WERs < 1 nm/min)[15] in dilute HF but only at high temperatures (>700 °C).[14] Using PECVD can lower the process temperatures to ~400 °C, but the SiN_x films exhibit a reduced conformality on 3D structures or imprecise film thickness control.[25] Thermal and plasma-enhanced atomic layer deposition (ALD, PEALD) are well-known methods for depositing high quality thin films with excellent growth control.[26−29] However, growing highly conformal (>95%) and wet-etch resistant (WER < 1 nm/min) SiN_x films in high aspect ratio structures (HARS) at low deposition temperatures (<400 °C) is not trivial to achieve, not even with ALD.[30] Table 1 provides a brief summary of SiN_x ALD processes reported in the literature.

ALD of SiN_x has been frequently reported employing chlorosilane precursors (such as $SiCl_4$, SiH_2Cl_2, Si_2Cl_6, and Si_3Cl_8) in combination with coreactants such as NH_3, NH_3 plasma, or N_2H_4.[15,31−37] Some of these processes have also reported on the attainment of highly conformal (>80%) SiN_x films when deposited on 3D substrates.[15,36,37] However, these processes generally require high temperatures for depositing high quality films as indicated by the low densities (<2.7 g/cm^3)[31,33,37] and high WER values (>10 nm/min)[15,36] reported for low temperature (<400 °C) growth conditions. Furthermore, halide containing precursors can lead to excessive particle formation, undesired incorporation of chlorine impurities, corrosive reaction byproducts, and incompatibility with metal substrates.[30,38] The use of silane or aminosilane precursors during PEALD can offer a halide-free deposition route.[38] King[25] employed both PECVD and PEALD processes to grow silicon nitride films on 3D trench structures (aspect ratio, AR ≈ 3.5:1) using silane (SiH_4) combined with N_2 plasma at low temperature (<400 °C). Film quality obtained was relatively low as indicated by the low mass densities (≤2.7 g/cm^3), while a conformality ≤50% was reported for the two processes. No WER values in dilute HF were reported. Triyoso et al.[14] carried out PEALD of SiN_x using trisilylamine ($N(SiH_3)_3$) combined with an H_2/N_2 intermixed plasma. The process yielded high quality films, represented by low WERs (≤1.5 nm/min) in dilute HF at deposition temperatures ≤400 °C. Good conformality was reported with side/top ratios of ~80%, but the 3D structures used were of a relatively low AR (~2:1). Trench structures with a higher AR (~5.5:1) used by Park et al.[39] gave a side/top ratio of ~73% for PEALD of SiN_x using a trisilylamine-derivative precursor ($N(SiHN(CH_3)_2CH_3)_2Si(CH_3)_3$) and N_2 plasma. WERs between 4.55 and 0.23 nm/min were reported but in a more diluted HF solution (HF/H_2O = 1:500). Recent work by Weeks et al.[40] reported a SiN_x PEALD process using neopentasilane ($Si(SiH_3)_4$) and N_2 plasma where they obtained films with low WER (~3 nm/min) in dilute HF but with low film densities (2.21 g/cm^3) for the optimized conditions. They also deposited SiN_x films on 3D trench structures with different AR values and observed a decrease in sidewall film thickness with depth inside the trench. Sidewall/top film thickness ratio was observed to be ~50% (within 200 nm of the top of the trench), similar to that of King,[25] irrespective of trench AR or increase in precursor dose (from 1 to 3 s) and plasma exposure (from 2 to 15 s).[40] They also observed soft saturation of GPC as a function of N_2 plasma exposure time, which indicates long cycle times similar to that of King[25] could be needed for saturation.

In previous work conducted within our group, Knoops et al.[16] developed a SiN_x process employing a bis(*tert*-butylamino)silane (BTBAS, $SiH_2(NH^tBu)_2$) precursor, depicted in Figure 1a, in combination with a remote N_2 plasma.

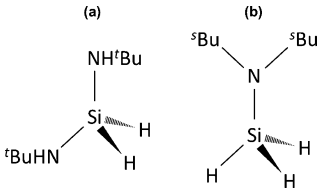

Figure 1. Schematic illustrations depicting the chemical constituents of (a) BTBAS and (b) DSBAS precursor molecules.

High quality SiN_x films were deposited having reasonable impurity contents ([C] < 10 at. % and [O] < 5 at. %). Moreover, the H content was relatively low ([H] < 11 at. %), and a low WER (~0.2 ± 0.5 nm/min at 400 °C) was obtained in dilute HF solution.[16] Insights provided by Ande et al.[41] later demonstrated that the growth rate of SiN_x using BTBAS is strongly reduced when NH_3, N_2 + H_2, or H_2 plasmas were used. This explained the choice of using an N_2 plasma over other H-containing plasmas as the coreactant during PEALD with BTBAS. In other studies related to this work, Knoops et al.[42] identified parameters governing the quality of SiN_x films deposited using BTBAS and N_2 plasma, while Bosch et al.[43] investigated the surface chemistry of that process with in situ infrared spectroscopy. They demonstrated that t-butylamine

DOI: 10.1021/acsami.6b12267
ACS Appl. Mater. Interfaces 2017, 9, 1858−1869

(NH^tBu) ligands remained on the surface after BTBAS adsorption and that these ligands get dissociated into fragments (C, H, and N species) during the subsequent N_2 plasma step. Redeposition of these fragments on the growing film surface leads to significant impurity contents in the deposited SiN_x films, which could be minimized by lowering the residence time of the plasma species.[42] This residence time was, therefore, identified as a key parameter governing film quality.[42] A high pumping capacity, together with adequately high gas flows and low plasma pressures, was demonstrated as a means for reducing the residence time of the species, which lowers redeposition and hence improves film quality (i.e., low WER ≈ 0.5 nm/min).[42] On the basis of these results, another route for minimizing redeposition can be hypothesized that may lead to high quality SiN_x films. Since the dissociation of ligands remaining on the surface after precursor adsorption was shown to cause redeposition, reducing or (ideally) eliminating the presence of such ligands on the surface before plasma exposure could, in principle, reduce or eliminate redeposition. Since the use of a *bis*-aminosilane precursor (with two amino ligands) has been shown to leave amino ligands on the surface,[43] the use of a *mono*-aminosilane precursor (with one amino ligand) could, in principle, leave fewer or (ideally) no amino ligands on the surface after precursor adsorption. As a result, comparatively fewer ligands would dissociate during plasma exposure after a *mono*-aminosilane precursor dose, thereby reducing impurity redeposition and improving film quality.

To validate this hypothesis, a new PEALD process for SiN_x was developed and studied in this work using the *mono*-aminosilane precursor di(*sec*-butylamino)silane (DSBAS, $SiH_3N(^sBu)_2$)[38,44−46] and N_2 plasma. The DSBAS molecule contains only one amino ligand, as depicted in Figure 1b. Material properties of SiN_x films deposited on planar substrate topographies have been compared with those obtained in our previous work[16] for films deposited using BTBAS and N_2 plasma. High-quality films with low [C], [O], and [H] levels and a high film density (~3.1 g/cm^3) were obtained on planar substrates at low substrate temperature (<400 °C) using DSBAS and N_2 plasma. WERs in dilute HF reported for SiN_x ALD processes discussed above are for films deposited on planar substrate topographies, which are not representative for assessing etch resistance within the 3D topographies incorporated in state-of-the-art device architectures. The process developed in this work with DSBAS was used to deposit SiN_x films on high aspect ratio (4.5:1) trench nanostructures to investigate film conformality and HF-etch resistance at different regions (planar and vertical sidewall) of the 3D substrate, relevant for modern device fabrication. Film conformality was observed to be low (≤50%) but comparable to values obtained for similar processes[25,40] reported in the literature. Yet, very low WERs were obtained at different regions of the trench nanostructures for the films deposited at low substrate temperature (<400 °C), which confirmed that the process is applicable for growing HF-etch resistant SiN_x on both planar and 3D substrate topographies.

EXPERIMENTAL DETAILS

PEALD of SiN_x. PEALD of SiN_x was performed using an Oxford Instruments FlexAL reactor.[47] It is equipped with a remote inductively coupled (ICP) plasma source, which was operated at 600 W of radio frequency power at 13.56 MHz and controlled by an automated matching network. The source consists of a water-cooled copper coil wrapped around a cylindrical alumina plasma tube. A base pressure in the reactor chamber of ~10^{-6} Torr was obtained using a turbo pump. A butterfly valve in front of the turbo pump controlled the effective pumping speed and functioned as an automated pressure controller (APC). The chamber wall temperature was set to 150 °C, except for instances where the deposition temperatures were below 150 °C, during which the wall was set to the deposition temperature. Due to poor thermal contact in vacuum, the actual temperatures of the substrates (wafer, coupon, see ALD film growth section) were lower than the set temperature of the substrate stage/table. This set temperature (henceforth referred to as stage temperature) can be fixed to a value between 25 and 500 °C. An estimation of the actual substrate temperature as a function of stage temperature is given in the Supporting Information. All substrates underwent a 30 min heating step prior to commencing deposition to ensure substrate temperature stabilization. DSBAS (assay ≥99.3%, see Supporting Information), synthesized and provided by Air Products and Chemicals Inc., was used as the precursor and held at a bubbler temperature of 40 °C. During precursor dosage, DSBAS was vapor drawn into the reaction chamber using Ar (25 sccm, purity 99.999%) as a carrier gas in the delivery line, with the APC valve completely closed. A reaction step was employed immediately after precursor dosage with the APC valve set to 10° to reduce the effective pumping speed and maximize precursor usage by confining it within the chamber. Setting the APC valve to 10° (i.e., almost closed) was necessary because a continuous flow of inert N_2 gas (50 sccm, purity 99.9999%) was passed through the alumina plasma tube during all process steps to reduce precursor adsorption on the inner surfaces of the tube during precursor dose and reaction steps. For both purge steps, the APC valve was fixed to a 90° valve position (i.e., fully open) for maximum pumping while 50 sccm of N_2 gas flowed through the alumina tube. The precursor delivery lines were heated to 70 °C to prevent precursor condensation and were purged with 100 sccm of Ar to remove any residual gas from previous ALD cycles.

PEALD Process Conditions. On the basis of the saturation curves for precursor dosage and plasma exposure obtained during process development using DSBAS and N_2 plasma (see ALD film growth section), the following step sequence was chosen as a standard PEALD recipe for SiN_x: 1 s delivery line purge, 100 ms DSBAS dose time, 3 s reaction time, 1 s precursor purge time, 2 s preplasma time (gas stabilization prior to plasma ignition), 10 s plasma exposure time, and 1 s plasma purge time. The 100 sccm N_2 gas flow and 12 mTorr pressure conditions were used for the plasma exposure step. These are outlined in Table 2. The standard PEALD recipe used for the previously reported PEALD process using BTBAS and N_2 plasma[16] is also outlined in Table 2 for comparison. For investigating conformality, additional runs using extended precursor dose times of 500, 1000, and 2000 ms and plasma exposure times of 20, 40, and 80 s were performed. These additional runs were initially based on previous Monte Carlo simulations on conformality by Knoops et al.[48] and then further extended based on the results observed. Extended precursor purge time of 3 s and plasma purge time of 2 s were also implemented

Table 2. Standard Parameters for the Previously Developed BTBAS Process[16] and the DSBAS Process Developed in This Work

process parameters	precursor	
	BTBAS	DSBAS
bubbler temperature (°C)	50	40
precursor dose time (ms)	150	100
plasma (N_2) exposure time (s)	10	10
precursor reaction step (s)	3	3
precursor purge time (s)	1	1
plasma purge time (s)	1	1
plasma (N_2) pressure (mTorr)	40	12
plasma (N_2) gas flow (sccm)	100	100

DOI: 10.1021/acsami.6b12267
ACS Appl. Mater. Interfaces 2017, 9, 1858−1869

for the additional conformality runs to account for any CVD component that could arise in the extended PEALD recipes.

Material Analysis and Characterization. SiN_x films were deposited on planar c-Si substrates with a thin native oxide layer (~1.5 nm) for developing the PEALD process. The optical properties and film thickness of the deposited layers on c-Si substrates were measured using spectroscopic ellipsometry (SE). Ex situ SE measurements were conducted using a J.A. Woollam Variable Angle SE with a VB-400 Control Module and an HS-190 Monochromator (1.2−6.5 eV). In situ SE measurements were performed in vacuum at an incidence angle of 70° (1.2−5 eV). The optical model used consisted of a silicon substrate, ~1.5 nm native oxide, and a silicon nitride layer fitted with a Cauchy dispersion relation in the optically transparent region for SiN_x (1.2−4 eV). The surface roughness was assumed negligible for these PEALD films. Rutherford backscattering spectrometry (RBS) and elastic recoil detection (ERD) measurements were used to determine the film composition (stoichiometry) and mass density of SiN_x deposited on planar c-Si substrates. The RBS and ERD measurements with subsequent data simulations were performed by AccTec B.V. and Detect 99 using a 1.8−2 MeV helium-ion beam. The areal densities of the elements were determined from raw data simulations. SiN_x film composition on the planar c-Si substrates was also investigated with X-ray photoelectron spectroscopy (XPS) measurements using a Thermo Scientific K-Alpha spectrometer equipped with a Al Kα X-ray source ($h\nu$ = 1486.6 eV). Note that the sensitivity factors, which are required for obtaining elemental concentrations, were previously determined for the XPS system used. Depth profiles were measured by sputtering with Ar^+ ions.

For investigating film conformality and wet-etch resistance on 3D substrate topographies, SiN_x layers were deposited using PEALD on coupons containing high aspect ratio trench nanostructures (width ~100 nm, height ~450 nm, AR = 4.5:1) and analyzed with cross-sectional TEM. These 3D nanostructures were created[37] by first depositing a thick SiO_2 film on a Si wafer using PECVD, which was subsequently etched into trench structures. The SiO_2 trench structures were then coated with a SiN_x layer using high-temperature CVD, on which a SiO_2 layer was deposited using ALD. Coupons containing these trench based HARS were prepared and provided by Lam Research. A JEOL 2010F ultrahigh-resolution scanning TEM at 200 kV was employed to obtain cross-sectional images of the SiN_x films deposited on the 3D trench nanostructures. The films were coated with a layer of spin-on epoxy to protect them from damage during sample preparation for TEM cross-sectional imaging. The samples were then placed on a Cu TEM grid, after which an energetic ion beam was used to mill and polish the samples at 30 kV, 100 pA and 5 kV, 40 pA, respectively. SiN_x film thickness was measured at three regions of several trench nanostructures in the sample, namely at the planar top and bottom regions together with the vertical bottom-side region (Conformality section, Figure 6A) by counting pixels in the TEM image. Conformality was determined by taking the ratio of SiN_x film thicknesses at the bottom-side and bottom of the trench to that at the top of the trench. The conformality values reported are the averages of the results obtained across several trench nanostructures with the same aspect ratio. Uncertainties reported for the values were based on both the accuracy of the measurement and the variation between measurements conducted across several trench nanostructures of the same sample.

For obtaining wet-etch rates (WER) of films at planar and vertical surfaces of the 3D substrates, coupons containing the trench nanostructures with SiN_x films deposited using PEALD were dipped in a dilute HF solution (HF/H_2O = 1:100) for 30 s. Two samples for TEM cross-sectional imaging were prepared from the same coupon, one before and one after the chemical wet-etch treatments. TEM measurements were conducted at the three aforementioned regions across several trench nanostructures of the same as-deposited and post wet-etch samples. The WERs at the aforementioned trench regions were determined by comparing the as-deposited and post wet-etch film thicknesses at those regions. The WER values reported are the average of the results obtained across several trench nanostructures with the same aspect ratio. Uncertainties reported for the values were based on both the accuracy of the measurement and the variation between measurements conducted across several trench nanostructures of the same sample. The WER and conformality values obtained using TEM for SiN_x deposited on trench nanostructures were used as a basis for determining film quality and thickness uniformity at planar and vertical surfaces of the 3D substrates. Potential depletion of the etchant inside the trench was not taken into account in these experiments.

RESULTS

PEALD of SiN_x on Planar Substrates. *ALD Film Growth.* Growth per cycle (GPC) values as a function of precursor dose time and plasma exposure time measured using in situ SE are shown in Figure 2a and b, respectively. GPC as a function of precursor purge and plasma purge times are also shown in Figure 2c and d, respectively. An apparent saturation for the GPC (~0.08 Å) can be observed in Figure 2a for the precursor dose time. The GPC using DSBAS is relatively low (<0.1 Å), and its rapid stagnation as a function of dose time suggests that the precursor quickly occupies the available reactive surface sites. Contrary to this apparent saturation behavior, the GPC as a function of N_2 plasma exposure time shows a soft saturation behavior (Figure 2b). This differs from the corresponding trend of GPC for the SiN_x PEALD process developed by Knoops et al.[16] using BTBAS. The GPC in that process peaked for short N_2 plasma exposure times and then gradually decreased to a constant value as the plasma exposure times were increased. Despite the nonideal soft saturation observed using DSBAS, SiN_x film growth was linearly dependent on the number of ALD cycles, while showing almost no nucleation delay, depicted in Figure 3. The slope of the plots is observed to decrease with temperature indicating a lower GPC at higher temperatures (see Effect of Substrate Temperature section).

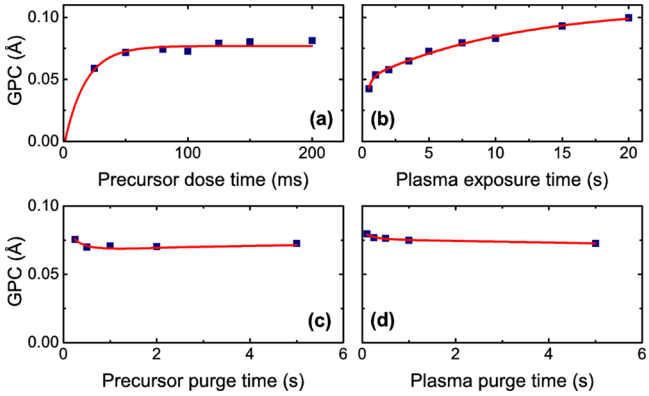

Figure 2. GPC as a function of (a) precursor dose time, (b) plasma exposure time, (c) precursor purge time, and (d) plasma purge time. The default precursor dose, plasma exposure, and purge times were 100 ms, 5 s, and 5 s, respectively. The red lines serve as a guide to the eye.

On the basis of these exploratory saturation experiments, a standard process was defined whose parameters were outlined in Table 2. Ideally, all process parameters are chosen assuming that the GPC saturates at a particular value. From Figure 2, it can be observed how a precursor dose time of 100 ms and purge times of 1 s can be expected to yield saturated film growth. The observed soft saturation of the GPC as a function of the plasma exposure time implies that very long exposures (≥20 s) would result in film growth closer to saturation. This would result in long cycle times (≥30 s), which, considering the

DOI: 10.1021/acsami.6b12267
ACS Appl. Mater. Interfaces 2017, 9, 1858−1869

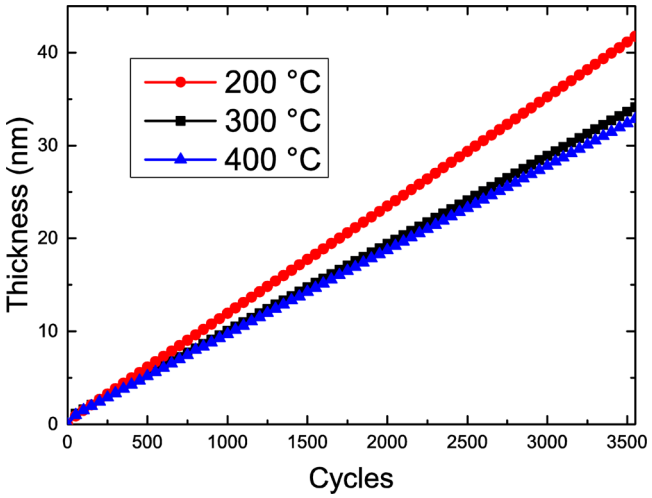

Figure 3. Film thickness as a function of the number of ALD cycles, as measured with in situ spectroscopic ellipsometry (SE) for three different stage temperatures (200, 300, and 400 °C).

already low GPC, would eventually lead to a long deposition time (~20 h) to grow SiN_x films of ~30 nm (roughly the target thickness required for accurate material characterization via RBS, see Table 3). As a result, a plasma exposure time of 10 s was chosen for the standard process to obtain a feasibly productive cycle time (~20 s).

Effect of Substrate Temperature. SiN_x film growth using DSBAS and N_2 plasma has been confirmed over a wide range of stage temperatures between 100 and 500 °C. This approximately corresponds to lower actual substrate temperatures[16] ranging between 100 and 360 °C (see Table 3 and Supporting Information). Film growth and material properties have been characterized at several temperatures in this range. The results are outlined in Table 3 and graphically depicted in Figure 4. The growth properties are presented in terms of both the film thickness deposited per cycle (Figure 4a) and the number of silicon atoms deposited per nm^2 per cycle (Figure 4b). The material properties are shown in terms of the N/Si ratio (Figure 4c), mass density (Figure 4d), and impurity content (Figure 4e and f). Note that the results obtained using DSBAS in this work are presented in Figure 4 with the results obtained in previous work for SiN_x deposited using BTBAS and N_2 plasma[16] to facilitate comparison between the material properties of films grown using the two processes.

Figure 4a shows how DSBAS yielded a fairly low, but constant film GPC (~0.1 Å) at various stage temperatures, with the exception of 100 °C where the GPC was higher (~0.2 Å). This increase in GPC is partly attributed to an increased impurity content ([C], [O], and [H]) at lower stage temperatures, as observed in Figure 4e and f.

Figure 4b shows the number of deposited Si atoms per nm^2 per cycle, denoted as GPC [Si] (Si at./nm^2). Since the only source of silicon is the one Si-atom present in both precursor molecules, GPC [Si] can be considered as a more quantitative measure of precursor adsorption. Like GPC, the values for GPC [Si] using DSBAS remain fairly unchanged at ~0.4 Si at./nm^2 with an increasing stage temperature. Both GPC and GPC [Si] are observed to be higher using BTBAS compared to those obtained using DSBAS at the standard conditions investigated for the two precursors. The differences are more pronounced at lower stage temperatures, while at 500 °C, they have been greatly reduced. The fairly unchanging trend in GPC and GPC [Si] exhibited by DSBAS differs from the trend observed for films grown using BTBAS where GPC and GPC [Si] monotonically decrease as a function of increasing stage temperature.

From Figure 4c, it can be observed that the N/Si ratio for films deposited using DSBAS is very close to that of stoichiometric Si_3N_4 (1.33), especially at 300 and 400 °C (1.3 and 1.4, respectively). At both low (≤200 °C) and high (500 °C) stage temperatures, more nitrogen-rich SiN_x films were deposited. The highest mass density of 3.1 g/cm^3 was obtained at a stage temperature of 500 °C, as seen in Figure 4d, even though the film was more nitrogen-rich in composition at that temperature. The highest obtained density is very close to the mass density of bulk Si_3N_4 (~3.2 g/cm^3).[49] The high refractive indices, close to 2.0, measured using ex-situ SE at stage temperatures >300 °C (shown in Table 3) also indicate high film quality.

The high quality is further corroborated by the low impurity content ([C], [O], and [H]) of the DSBAS grown films, especially at stage temperatures >200 °C. At 500 °C, both [C] and [O] levels have decreased to values below the detection limit of 2% and 1%, respectively. However, at 100 °C, the [C] and [H] levels were significantly higher (11% for both) compared to those at higher temperatures (>200 °C), as observed in Figure 4e and f, respectively. The film density at 100 °C is quite low (~2.3 g/cm^3), which is most likely due to the aforementioned high [C] and [H] levels together with

Table 3. GPC, Refractive Index at 2 eV, Mass Density, and Elemental Composition of ~30 nm Thick SiN_x Films Deposited Using Standard 100 ms DSBAS Precursor Dose and 10 s N_2 Plasma Exposure Times at 12 mTorr N_2 Plasma Pressure and Various Stage Temperatures (100−500 °C)[a]

				RBS					ERD
stage temp. (°C)	estimated actual substrate temp. (°C)	GPC (Å)	refractive index	mass density (g/cm^3)	#Si at. per nm^2 per cycle	N/Si	[C] at. %	[O] at. %	[H] at. %
100	100 ± 20	0.19 ± 0.02	1.86 ± 0.05	2.3 ± 0.1	0.43 ± 0.02	1.9 ± 0.1	11 ± 2	2 ± 1[b]	11 ± 1
200	180	0.12	1.93	2.7	0.37	1.4	3	3	8
300	240	0.10	1.98	2.9	0.35	1.3	2	3	5
400	310	0.09	1.99	3.1	0.35	1.4	2	1	5
500	360	0.10	1.97	3.1	0.37	1.5	<d.l.[c]	<d.l.[c]	5

[a]Typical uncertainties are given in the first row. Bulk Si_3N_4 has a refractive index of 2.02 and a mass density of 3.2 g/cm^3.[49] [b]XPS measurements showed this film had a high level of oxygen at the surface, which is likely due to the low mass density of the film that leads to significant postdeposition oxidation (see Supporting Information). [c]Values below detection limit (d.l.) of 2% for [C] and 1% for [O].

DOI: 10.1021/acsami.6b12267
ACS Appl. Mater. Interfaces 2017, 9, 1858−1869

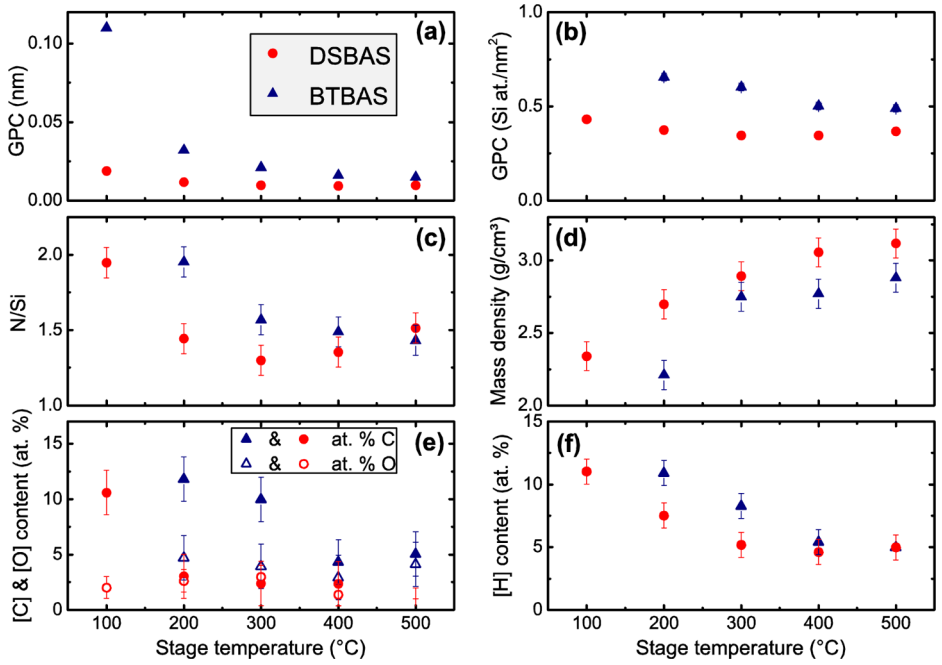

Figure 4. Material properties of SiN_x films deposited using DSBAS compared to those obtained previously using BTBAS.[16] Growth-per-cycle (GPC) in terms of (a) thickness, (b) the number of deposited silicon atoms per ALD cycle, (c) the nitrogen to silicon ratio N/Si, (d) the mass density, (e) the contents of carbon [C] and oxygen [O] in atomic %, and (f) hydrogen content [H] in atomic % as a function of stage temperature. Note that deposition conditions differ slightly for the BTBAS and DSBAS data series, primarily because of a difference in plasma pressure (12 mTorr for DSBAS, 40 mTorr for BTBAS). Results in panel a were obtained via spectroscopic ellipsometry (SE), in panels b–e via Rutherford backscattering spectrometry (RBS), and in panel f via elastic recoil detection (ERD).

postdeposition oxidation that the films may have undergone upon exposure to the atmosphere.

With respect to the high quality of films obtained previously using the BTBAS process, it can be concluded that the film quality yielded by the DSBAS process is generally very high. The density, N/Si ratio, and refractive index values of the DSBAS grown films tend to be closer to those of bulk Si_3N_4 compared to BTBAS grown films, with an exception for the higher N/Si ratio at 500 °C. The N/Si ratio trend for DSBAS differs from that for BTBAS, which shows a monotonic decrease in N/Si as a function of increasing stage temperature, as observed in Figure 4c. For the conditions investigated, it can be concluded that using DSBAS as a precursor for PEALD of SiN_x yields denser films with lower impurities, and hence higher quality films at all stage temperatures compared to using BTBAS as the precursor.

To verify whether SiN_x film composition remained uniform throughout the entire layer of the deposited films, depth profiles were measured using alternating XPS measurements and Ar^+ ion sputter steps. The constant N and Si atomic contents, as observed in Figure 5, indicate a uniform film stoichiometry (i.e., constant N/Si ratio) throughout the entire film thickness. Elevated [C] and [O] levels can be observed near the film surface, which indicate that some surface contamination takes place after the deposited films are exposed to the atmosphere.

Effect of Plasma Pressure. As mentioned before, the residence time is a key parameter that can influence the redeposition effect and hence govern growth properties and material quality during PEALD.[42] Since the residence time was shown to depend on plasma pressure, which was not the same for the two processes compared, the effect of similar plasma pressures on material properties of both BTBAS and DSBAS

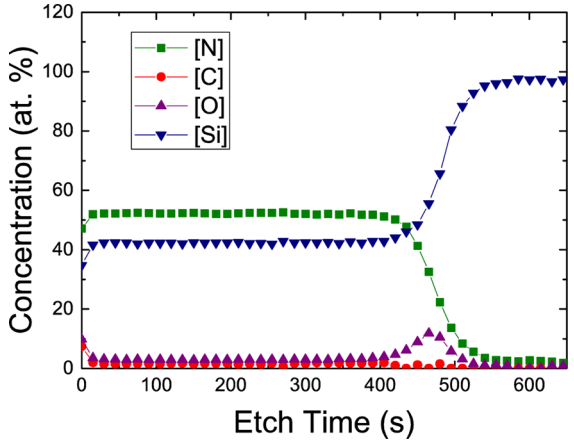

Figure 5. Depth profile of a SiN_x film deposited using DSBAS and N_2 plasma at a stage temperature of 400 °C, as determined by XPS. Minor oxidation and C contamination levels can be observed near the film surface. The native oxide layer present on the c-Si substrate shows up as an elevated O content at ~450 s.

grown SiN_x films was investigated (at stage temperature of 200 °C). These results are outlined in Table 4. The films deposited using DSBAS show higher refractive indices and lower impurity contents at both 12 and 40 mTorr compared to the films deposited using BTBAS at similar pressures. Furthermore, the GPC using BTBAS increased significantly when the plasma pressure was increased from 13 to 40 mTorr, whereas the GPC using DSBAS remained unaffected. The [C] of the films deposited using both precursors increased with pressure, indicating elevated impurity content at higher plasma pressure.

PEALD of SiN_x on 3D Substrates. *Conformality.* TEM images of as-deposited SiN_x layers grown on 3D trench

DOI: 10.1021/acsami.6b12267
ACS Appl. Mater. Interfaces 2017, 9, 1858–1869

Table 4. GPC, Refractive Index at 2 eV, Mass Density and Elemental Composition of ~30 nm Thick SiN_x Films Deposited at a Stage Temperature of 200 °C Using Standard Dose Times of 100 or 150 ms for the DSBAS or BTBAS Precursor Steps, Respectively[a]

				XPS			RBS					ERD
precursor	N_2 plasma pressure (mTorr)	GPC (Å)	refractive index	N/Si	[C] at. %	[O] at. %	mass density (g/cm^3)	#Si at. per nm^2 per cycle	N/Si	[C] at. %	[O] at. %	[H] at. %
BTBAS	13	0.24 ± 0.02	1.91 ± 0.05	1.6 ± 0.2	6 ± 2	5 ± 2	-	-	-	-	-	-
BTBAS	40	0.32	1.83	1.7	9	5	2.2 ± 0.1	0.66 ± 0.02	2.0 ± 0.1	12 ± 1	4 ± 1	11 ± 1
DSBAS	12	0.12	1.93	1.2	4	4	2.7	0.37	1.4	3 ± 2	3	8
DSBAS	40	0.12	1.89	1.2	5	7	2.7	0.37	1.5	6	4	8

[a]All films were deposited using 10 s N_2 plasma exposure times but at different pressures in the reactor during plasma exposure. Typical uncertainties are given in the first and second rows, unless otherwise noted. A "-" means not measured.

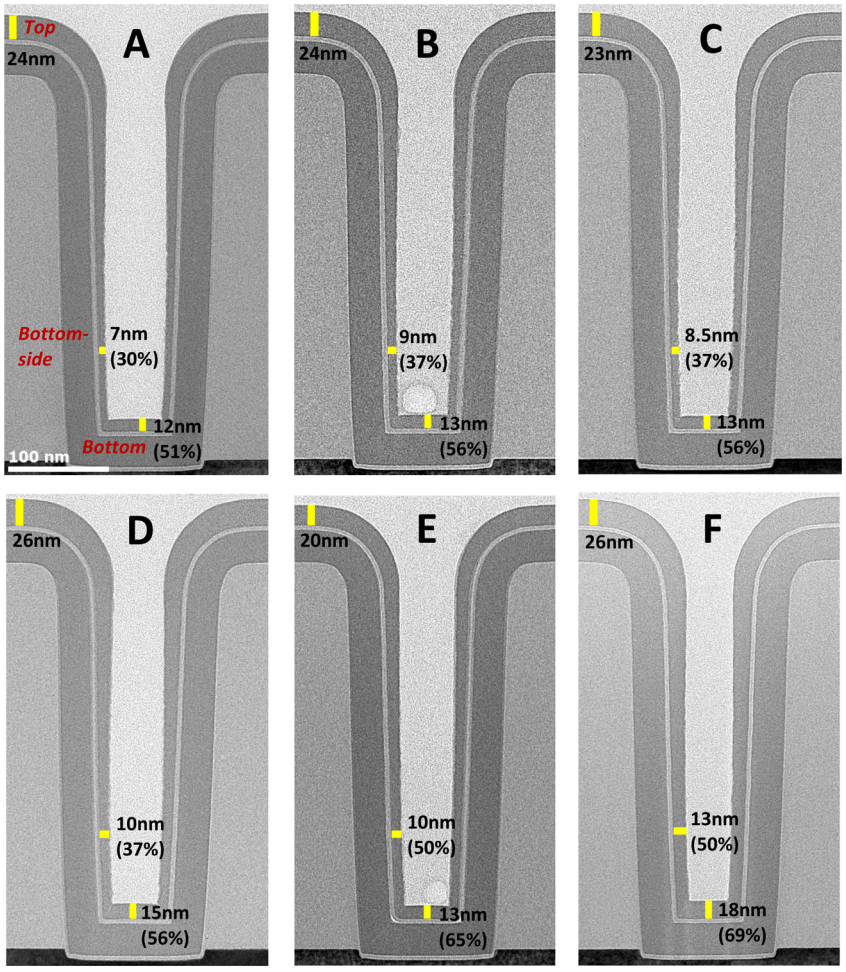

Figure 6. (A–F) TEM images of as-deposited SiN_x layers grown on 3D trench nanostructures (AR = 4.5:1) using DSBAS and N_2 plasma at 500 °C stage temperature and 12 mTorr plasma pressure. The deposition conditions for each image are outlined in Table 5. SiN_x film thicknesses for all depositions are measured at three regions of the trench, top, bottom-side, and bottom, as indicated in panel A. SiN_x film conformality at the bottom-side and bottom regions of the trench are indicated as a percentage of film thickness at the top in all panels.

nanostructures (AR = 4.5:1) using DSBAS and N_2 plasma are shown in Figure 6, and their corresponding deposition conditions are outlined in Table 5. SiN_x film thicknesses measured at the top, bottom-side, and bottom regions of the trench together with film conformality (as % of film thickness at the top) are also depicted in Figure 6 and Table 5. In the first experiment, the film was deposited on 3D trench nanostructures using the standard recipe of 100 ms DSBAS dose and 10 s N_2 plasma exposure at 500 °C stage temperature and 12 mTorr plasma pressure. These standard conditions yielded bottom-side and bottom conformalities of 30% and 51%, respectively, as shown in Figure 6A.

Using Monte Carlo simulations, Knoops et al.[48] showed that to reach 100% conformality in HARS, generally higher precursor doses and longer plasma exposures are needed compared to those used for obtaining saturation on planar substrates. On the basis of this and the low film conformalities exhibited by the standard recipe, extended precursor dose and plasma exposure times were used to deposit SiN_x films on the 3D trench nanostructures (Figure 6B–F). The conformalities

DOI: 10.1021/acsami.6b12267
ACS Appl. Mater. Interfaces 2017, 9, 1858–1869

Table 5. Conformality and Wet-Etch Rates of SiN_x Films Grown on Coupons Containing 3D Trench Nanostructures (AR = 4.5:1) Using DSBAS and N_2 Plasma at 500 °C Stage Temperature and 12 mTorr Plasma Pressure[a]

TEM image	precursor dose time (ms)	plasma exposure time (s)	TEM thickness at the top (nm)	as-deposited conformality (% of top)		wet-etch rate (nm/min)		
				bottom-side	bottom	top	bottom-side	bottom
A	100	10	24 ± 1	30 ± 5	51 ± 5	0 ± 1	1 ± 1	0 ± 1
B	100	20	24	37	56	0	1	0
C	500	10	23	37	56	0	6	2
D	500	20	26	37	56	0	3	1
E	1000	40	20	50	65	2	3	1
F	2000	80	26	50	69	0	2	1

[a]The wet-etch rates are reported for SiN_x films located at planar (top, bottom) and vertical (bottom-side) regions of the 3D substrate topographies after 30 s dip in an etchant solution of dilute hydrofluoric acid (HF/H_2O = 1:100). Typical uncertainties, which are based on both the accuracy of the measurement and the variation between measurements conducted across different trenches of the same coupon, are given in the first row.

improved slightly to 37% and 56% at the bottom-side and bottom, respectively, in accordance with the simulations[48] when either the precursor dose was extended to 500 ms (Figure 6C), or the plasma exposure to 20 s (Figure 6B), or both simultaneously (Figure 6D). Doubling both the precursor dose to 1000 ms and plasma exposure to 40 s (Figure 6E) significantly improved bottom-side and bottom film conformalities to 50% and 65%, respectively. This trend of continued improvement in film conformality by extending the durations of both PEALD half cycles was the reason to further double the precursor dose and plasma exposure times to 2000 ms and 80 s, respectively (Figure 6F). However, no further improvements were observed as film conformalities of 50% and 69% were obtained at the bottom-side and bottom regions of the trench, respectively, which was also the most conformal film obtained in this work.

Wet-Etch Rate. WERs for SiN_x films deposited on 3D trench nanostructures using DSBAS and N_2 plasma at 500 °C stage temperature (<400 °C actual substrate temperature) and 12 mTorr plasma pressure are outlined in Table 5. The WER values were determined by comparing the as-deposited and post wet-etch film thicknesses at the three trench regions depicted in Figure 6A. The deposited SiN_x films seem to be highly etch resistant at the planar top and bottom regions of the trench, as indicated by small or insignificant WER values (≤2 ± 1 nm/min) observed at those regions (Table 5). These low WERs indicate the deposition of high quality SiN_x films on planar or horizontal surfaces of the 3D trench nanostructures, as observed in Figure 6. This is also corroborated by the high mass density (3.1 g/cm^3) exhibited by the film deposited on a planar c-Si substrate using the standard deposition condition (100 ms DSBAS, 10 s N_2 plasma), as outlined in Table 3. Additional RBS measurements were conducted for two SiN_x films deposited on planar c-Si substrates using extended conditions (500 and 1000 ms DSBAS, 20 and 40 s N_2 plasma, respectively), which also showed high mass densities (~3.1 g/cm^3) and near-stoichiometric N/Si ratios (~1.4) for both films. This corroborates the low WERs that were also observed for SiN_x films deposited on 3D trench nanostructures using the extended deposition conditions. It is noted that the mass densities of the two SiN_x films deposited on planar c-Si substrates using extended precursor dose and plasma exposure conditions remained high even though slightly elevated [C] and [O] levels (~4% for both) were observed for the films at those conditions.

The WERs observed at the bottom-side region of the trench are somewhat higher than those at the two planar trench regions for all SiN_x films, indicating a reduced HF-etch resistance at the vertical trench surfaces. However, they are small in absolute magnitude (≤3 nm/min) indicating a high HF-etch resistance for all SiN_x films for both planar and vertical surfaces. Only the film deposited using 500 ms DSBAS dose and 10 s N_2 plasma exposure (Table 5, TEM image C) is an exception. The bottom-side WER for this particular film is significantly high (~6 nm/min), and the film was deposited after only the precursor dose time was extended from 100 to 500 ms in the standard recipe, without extension of the plasma exposure time. When the plasma exposure time was also extended from 10 to 20 s for the extended 500 ms precursor dose (Table 5, TEM image D), the WER was seen to decrease (~3 nm/min). This indicates that an increased precursor dose requires a corresponding increase in plasma exposure in order for the SiN_x films to retain their etch resistance at the vertical surfaces within a 3D structure. A high film quality was observed in general with the lowest WERs (≤2 nm/min) exhibited by the standard (100 ms DSBAS, 10 s N_2 plasma) and the most extended (2000 ms DSBAS, 80 s N_2 plasma) deposition conditions, as seen in Figure 7. The most extended deposition condition resulted in optimum SiN_x having both low WERs and the highest conformality on 3D trench nanostructures in this work. WERs at the regions inside a trench nanostructure (bottom-side and bottom) were always higher than the region at the trench entrance (top). Although any potential depletion of etchant inside the trench was not taken into account, the comparatively higher WERs at the regions inside the trench ensured etchant penetration to the bottom of the trench nanostructures. Furthermore, nonexistence of lower WERs at the regions inside the trench indicated the absence of any delay in wetting of the etchant on the film surfaces within the trench. Therefore, the wetting of the etchant was assumed to occur instantaneously relative to the large time scale (30 s) of the etch treatment.

DISCUSSION

PEALD of SiN_x on Planar Substrates. The results on planar substrates indicate that high quality SiN_x films with properties relatively close to that of bulk Si_3N_4[49] can be obtained using DSBAS as the precursor for PEALD of SiN_x. This is demonstrated by stoichiometric N/Si ratios (between 1.3 and 1.5), high mass densities (>2.9 g/cm^3), and low impurity contents ([C] < 2%, [O] < 3%, and [H] ≈ 5%) exhibited by the SiN_x films deposited at stage temperatures between 300 and 500 °C.

DOI: 10.1021/acsami.6b12267
ACS Appl. Mater. Interfaces 2017, 9, 1858−1869

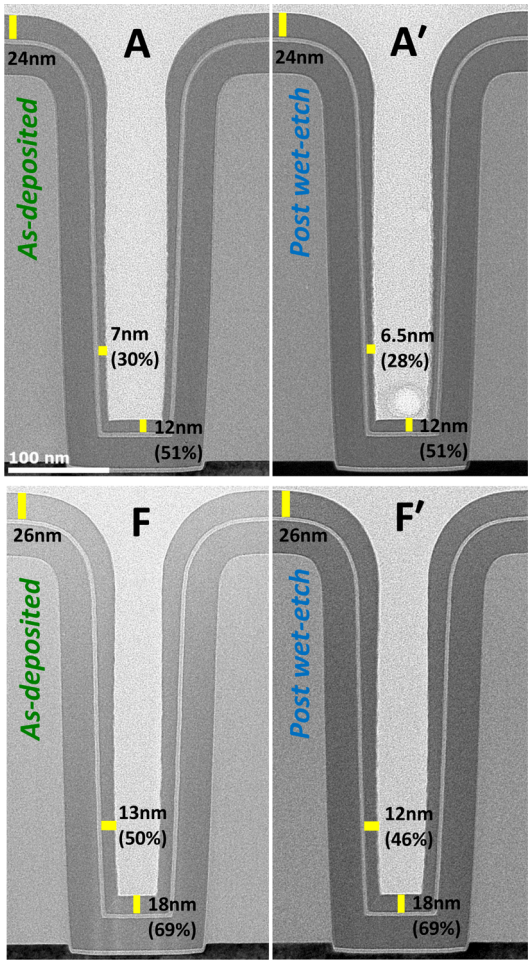

Figure 7. TEM images of (A, F) as-deposited and (A′, F′) post wet-etch (in 30 s dilute HF) SiN_x films grown on 3D trench nanostructures (AR = 4.5:1) using DSBAS and N_2 plasma at 500 °C stage temperature and 12 mTorr plasma pressure. The deposition conditions for panels A and F are outlined in Table 5. SiN_x film conformality at the bottom-side and bottom regions of the trench are indicated as a percentage of film thickness at the top in all panels.

In Figure 2b, the GPC as a function of N_2 plasma exposure time was seen to exhibit soft saturation using DSBAS as the precursor for depositing SiN_x. The GPC was modeled by fitting two exponential functions involving two different time constants, $\tau_1 \approx 0.3$ s and $\tau_2 \approx 11$ s (see Supporting Information). This indicates that the creation of reactive sites slowed down but did not completely stop with increase in N_2 plasma exposure time. The exact nature of these reactive surface sites is not clear at the moment. Previous studies conducted using density functional theory (DFT) have shown that precursor adsorption is promoted on undercoordinated surface sites such as nitrogen dangling bonds.[41] Both experimental results and first-principles calculations reported by Ande et al.[41] indicated that the use of an N_2 plasma can generate such undercoordinated surface sites, which are speculated to be the reactive sites on which DSBAS adsorption occurs in this work. Similar soft saturation of GPC as a function of N_2 plasma exposure has been recently reported by Weeks et al.[40] for PEALD of SiN_x using neopentasilane and trisilylamine as precursors. Both precursor molecules are terminated by silyl (SiH_3) groups, which could give rise to a $Si-H_x$ terminated surface after precursor adsorption. The DSBAS molecule also consists of a silyl group (and one amino ($N(^sBu)_2$) ligand, as shown in Figure 1b) in addition to exhibiting a similar soft saturation behavior during N_2 plasma exposure. On the basis of these similarities, it could be speculated that DSBAS precursor adsorption following an N_2 plasma step results in a surface closely resembling a $Si-H_x$ terminated surface, which is generated by the two aforementioned SiH_3 terminated precursors. Such a surface could be generated by the one-step elimination of the sole amino ligand during DSBAS adsorption that has been reported to occur for ALD processes employing this precursor.[38,50]

On the other hand, when BTBAS was used as the precursor for depositing SiN_x in previous work,[16] the GPC as a function of N_2 plasma exposure time exhibited a different behavior from soft saturation. The GPC was reported to undergo an initial rapid overshoot followed by a gradual decrease to a constant (or saturated) value as the N_2 plasma exposure time was increased.[16] Unlike the DSBAS molecule, which has one amino ligand and a silyl group, the *bis*-aminosilane BTBAS molecule consists of two amino (NH^tBu) ligands and a silanediyl (SiH_2) group, as shown in Figure 1a. DFT studies on the surface chemistry of BTBAS during ALD have shown that it involves the sequential elimination of primary and secondary NH^tBu ligands,[51,52] while DSBAS undergoes the elimination of just one $N(^sBu)_2$ ligand.[38,50] Experimental studies on the surface chemistry of the SiN_x ALD process employing BTBAS and N_2 plasma[43] confirmed that a part of the amino ligands are liberated as gas-phase $NH_2{}^tBu$ species during BTBAS adsorption, while a part remains on the surface as NH^tBu. Consequently, BTBAS precursor adsorption can be considered to generate a more amino ligand terminated surface compared to a more $Si-H_x$ (or conversely, amino ligand deficient) surface hypothesized earlier for DSBAS. Previous work by Knoops et al.[42] and recent investigation by Bosch et al.[43] demonstrate that the amino ligands remaining on the surface after a BTBAS precursor step get dissociated into reactive fragments (e.g., C_2N_2, C_3H_8, HCN, etc.) during the subsequent N_2 plasma step. These fragmented ligand species can then be redeposited as impurities on the growing film surface, which is manifested as the initial rapid overshoot in GPC reported for BTBAS,[16] but not observed in this work for DSBAS. As a result, the NH^tBu terminated surface after BTBAS adsorption could undergo a more prominent redeposition effect during N_2 plasma exposure compared to the more amino ligand deficient surface speculated for DSBAS. This may explain the lower total GPC (Figure 4a), smaller impurity content ([C] and [H], Figure 4e,f), and consequently higher film density (Figure 4d) observed for SiN_x films deposited using DSBAS compared to previous results obtained using BTBAS.

The one-step ligand elimination process for DSBAS[38,50] entails overcoming a single energy barrier compared to the two-step counterpart process for BTBAS[51,52] where two energy barriers need to be overcome. The sequential two-step ligand elimination for BTBAS may be incomplete at low temperatures causing more NH^tBu ligands to remain on the surface after BTBAS dosage. Conversely, fewer amino ligands may be left on the surface after a precursor dose step using DSBAS instead of BTBAS, with the difference becoming more prominent on decreasing the stage temperature. The more amino ligands remaining on the surface after precursor adsorption, the greater the extent of ligand fragmentation during plasma exposure and the larger the effect of redeposition. Species that redeposit on the surface can be again removed by the plasma, and these

DOI: 10.1021/acsami.6b12267
ACS Appl. Mater. Interfaces 2017, 9, 1858−1869

redeposition and removal processes occur continuously until the fragmented species are flushed out of the reaction chamber.[42] High temperatures could be speculated to enhance the removal process by facilitating thermal desorption of redeposited species, while low temperatures could have the opposite effect and lead to more impurity redeposition. This may account for the significantly higher impurity contents ([C] and [H], Figure 4e,f) observed at low stage temperatures (<300 °C) using BTBAS that results in a much lower film density (Figure 4d) and a more elevated total GPC (Figure 4a) compared to DSBAS. Conversely, thermally enhanced desorption of redeposited species or a more complete two-step ligand elimination process may occur for BTBAS at high temperatures (>300 °C), which lowers redeposition and leads to SiN_x film properties approaching those observed for DSBAS.

PEALD of SiN_x on 3D Substrates. SiN_x films deposited on 3D trench nanostructures (AR = 4.5:1) using standard DSBAS and N_2 plasma conditions (Table 5, TEM image A) yielded suboptimal bottom-side and bottom conformalities (30% and 51%, respectively, Figure 6A). This indicates that the film GPCs at the bottom-side and bottom regions of the 3D trench nanostructures were significantly lower than the GPC at the top. Increases in precursor dose and plasma exposure times were subsequently implemented with the aim of ensuring film GPC, and consequently film thickness, were the same at all regions of the trench nanostructures. Simultaneously extending both precursor dose and plasma exposure conditions (Table 5, TEM images D and E) seemed to offer a route toward improving bottom-side and bottom film conformalities (Figure 6D,E). However, this trend did not continue at a certain point when further extension in both precursor dose and plasma exposure times (from 1000 to 2000 ms and 40 to 80 s, respectively) no longer improved bottom-side and bottom conformalities (Figure 6E,F). This observation can potentially be explained by the combined role played by three factors during SiN_x deposition on such 3D substrates.

A part of the reason could be due to the previously mentioned aspect of soft saturation observed for the GPC as a function of N_2 plasma exposure time. A continued increase in SiN_x film growth rate was observed when the N_2 plasma exposure time was increased to 40 and 80 s. This may cause the GPC at the top to exceed those at the bottom-side and bottom regions of the trench nanostructures and thereby yield nonconformal films. Another reason could be due to the recombination of growth species at the vertical surfaces near the top of the trench. The ALD process developed in this work for depositing SiN_x is an N_2 plasma based process, whereby atomic N radicals generated in the plasma are deemed as important contributors toward film growth.[25] These charge-free N radical species are isotropic or nondirectional in nature, which means that they can collide and recombine at the vertical surfaces of the trench nanostructures before they reach the bottom regions of the trench. Kessels et al.[53,54] estimated the recombination loss probability of N radicals on SiN_x surfaces to be of the order of $\sim 10^{-2}$. Knoops et al.[48] identified that recombination losses of plasma radicals at the surfaces within a HARS during PEALD can lower the radical flux at the bottom regions of the HARS. This means that the flux of growth species composed of N radicals is reduced at the bottom regions of the 3D trench nanostructures, which causes film GPC in those regions to be lower than that at the top. This GPC discrepancy between the top and bottom regions of the trench lowers film conformality. Finally, anisotropic ion bombardment, which is a distinct feature of plasma ALD processes at such low pressures,[27] can also play a role behind the low conformalities. N_2^+ ions generated in the plasma are charged species that are accelerated vertically downward by the plasma sheath formed above the substrate. This vertically directed or anisotropic nature of N_2^+ ion bombardment can preferentially generate more reactive sites on the planar or horizontal surfaces of 3D trench nanostructures than on the vertical sidewalls. Therefore, the GPCs at the planar surfaces exceed those at the vertical ones which subsequently lowers film conformality within the 3D trench nanostructures. Similar low conformalities were also observed by King[25] and Weeks et al.[40] who also used N_2 plasma for PEALD of SiN_x on 3D trench nanostructures. Both works also attributed the low conformalities to the anisotropic nature of N_2^+ ion bombardment.

Despite the low conformalities, high quality SiN_x films were obtained, which were demonstrated by the low WERs exhibited by nearly all the films deposited on 3D trench nanostructures. The WERs at the vertical trench sidewalls are slightly higher than those at the planar or horizontal trench surfaces. This could be due to the anisotropic nature of N_2^+ ion bombardment, which preferentially improves film properties at horizontal surfaces more than those at vertical ones. The trade-off between high conformality and high quality (i.e., low WERs, high density) observed for SiN_x films deposited on 3D substrate topography in this work seems to be a generally observed phenomenon for ALD processes of SiN_x.[55,56] Processes employing chlorosilane precursors and NH_3 gas or NH_3 plasma report films having high conformality but low film quality (i.e., high WERs, low density),[15,36,37] whereas those using an organosilane precursor and N_2 plasma report films with the properties reversed.[25,40] The latter is consistent with the results obtained in this work.

CONCLUSIONS

A new PEALD process for SiN_x was developed using DSBAS and N_2 plasma. Material properties were analyzed over a wide stage temperature range (100−500 °C) and compared with those obtained in our previous work for SiN_x deposited using BTBAS and N_2 plasma. High-quality films were obtained on planar substrates using DSBAS and N_2 plasma, with the best films showing high density (~3.1 g/cm^3) approaching that of bulk Si_3N_4 and low [C], [O], and [H] impurity levels at low substrate temperature (<400 °C). DSBAS, having one amino ligand and a silyl group, is hypothesized to leave a more amino ligand deficient surface after precursor adsorption compared to BTBAS that has two amino ligands and a silanediyl group. As a result, a lower redeposition effect during the subsequent N_2 plasma step could take place for DSBAS, which could account for the denser SiN_x films having lower impurity contents compared to those obtained previously using BTBAS. The process developed using DSBAS was also used for depositing SiN_x films on high aspect ratio (4.5:1) 3D trench nanostructures. Film conformality is not yet at desired levels of >95% and is attributed to the combined role played by nitrogen plasma soft saturation, radical species recombination, or ion directionality during SiN_x deposition on 3D substrates. However, high-quality films were obtained on the 3D substrates as demonstrated by the low or insignificant wet-etch rates (WER ≤ 2 nm/min) observed at the top, sidewall, and bottom trench regions of the most conformal film deposited at low substrate temperature (<400 °C). These observations are in line with similar results reported in the literature employing

DOI: 10.1021/acsami.6b12267
ACS Appl. Mater. Interfaces 2017, 9, 1858−1869

organosilane precursors and N_2 plasma for ALD of SiN_x on 3D substrates.

■ ASSOCIATED CONTENT

Supporting Information

The Supporting Information is available free of charge on the ACS Publications website at DOI: 10.1021/acsami.6b12267.

Estimated actual substrate temperatures as a function of set temperature of substrate stage; purity of precursors discussed in this work; XPS depth profile analysis of SiN_x film deposited at 100 °C; outline of fitting parameters of N_2 plasma saturation curve presented in Figure 2b of this work (PDF)

■ AUTHOR INFORMATION

Corresponding Authors

*E-mail: t.faraz@tue.nl.

*E-mail: w.m.m.kessels@tue.nl.

ORCID

Tahsin Faraz: 0000-0001-8497-861X

Author Contributions

¶These authors contributed equally to this work.

Notes

The authors declare no competing financial interest.

■ ACKNOWLEDGMENTS

The authors would like to thank Cristian van Helvoirt and Jeroen van Gerwen for their invaluable assistance and guidance during this work. The research of one of the authors (W.M.M.K.) has been made possible by the Dutch Technology Foundation STW and The Netherlands Organization for scientific Research (NWO, VICI programma, 10817). Part of the work was carried out within the framework of the COST Action MP1402 – Hooking together European research in Atomic Layer Deposition (HERALD).

■ ABBREVIATIONS

DSBAS, di(*sec*-butylamino)silane; BTBAS, bis(*tert*-butylamino)silane; WER, wet-etch rate; HARS, high aspect ratio structure

■ REFERENCES

(1) King, S. W. Dielectric Barrier, Etch Stop, and Metal Capping Materials for State of the Art and beyond Metal Interconnects. *ECS J. Solid State Sci. Technol.* **2015**, *4* (1), N3029–N3047.

(2) *CMOS Nanoelectronics: Innovative Devices, Architectures, and Applications*; Collaert, N., Ed.; CRC Press: Boca Raton, FL, 2012.

(3) Choi, Y. K.; King, T. J.; Hu, C. Spacer FinFET: Nanoscale Double-Gate CMOS Technology for the Terabit Era. *Solid-State Electron.* **2002**, *46* (10), 1595–1601.

(4) Degroote, B.; Rooyackers, R.; Vandeweyer, T.; Collaert, N.; Boullart, W.; Kunnen, E.; Shamiryan, D.; Wouters, J.; Van Puymbroeck, J.; Dixit, A.; Jurczak, M. Spacer Defined FinFET: Active Area Patterning of Sub-20 nm Fins with High Density. *Microelectron. Eng.* **2007**, *84* (4), 609–618.

(5) Altamirano-Sánchez, E.; Tao, Z.; Gunay-Demirkol, A.; Lorusso, G.; Hopf, T.; Everaert, J.-L.; Clark, W.; Constantoudis, V.; Sobieski, D.; Ou, F. S.; Hellin, D. Self-Aligned Quadruple Patterning to Meet Requirements for Fins with High Density. *SPIE Newsroom* **2016**, 1 DOI: 10.1117/2.1201604.006378.

(6) Givens, J.; Geissler, S.; Lee, J.; Cain, O.; Marks, J.; Keswick, P.; Cunningham, C. Selective Dry Etching in a High Density Plasma for 0.5 μm Complementary Metal–oxide–semiconductor Technology. *J. Vac. Sci. Technol., B: Microelectron. Process. Phenom.* **1994**, *12* (1), 427.

(7) Auth, C.; Allen, C.; Blattner, A.; Bergstrom, D.; Brazier, M.; Bost, M.; Buehler, M.; Chikarmane, V.; Ghani, T.; Glassman, T.; Grover, R.; Han, W.; Hanken, D.; Hattendorf, M.; Hentges, P.; Heussner, R.; Hicks, J.; Ingerly, D.; Jain, P.; Jaloviar, S.; James, R.; Jones, D.; Jopling, J.; Joshi, S.; Kenyon, C.; Liu, H.; McFadden, R.; McIntyre, B.; Neirynck, J.; Parker, C.; Pipes, L.; Post, I.; Pradhan, S.; Prince, M.; Ramey, S.; Reynolds, T.; Roesler, J.; Sandford, J.; Seiple, J.; Smith, P.; Thomas, C.; Towner, D.; Troeger, T.; Weber, C.; Yashar, P.; Zawadzki, K.; Mistry, K. A 22nm High Performance and Low-Power CMOS Technology Featuring Fully-Depleted Tri-Gate Transistors, Self-Aligned Contacts and High Density MIM Capacitors. In *Digest of Technical Papers*, Proceedings of the Symposium on VLSI Technology, Honolulu, Hawaii, USA; June 12–14, 2012; IEEE, 2012; pp 131–132.

(8) Koehler, F.; Triyoso, D. H.; Hussain, I.; Antonioli, B.; Hempel, K. Challenges in Spacer Process Development for Leading-Edge High-k Metal Gate Technology. *Phys. Status Solidi* **2014**, *11* (1), 73–76.

(9) Triyoso, D. H.; Jaschke, V.; Shu, J.; Mutas, S.; Hempel, K.; Schaeffer, J. K.; Lenski, M. Robust PEALD SiN Spacer for Gate First High-k Metal Gate Integration. In *Proceedings of the International Conference on IC Design Technology (ICICDT)*, Austin, Texas, USA; May 30–June 1, 2012; IEEE, 2012; pp 1–4.

(10) Raaijmakers, I. J. Current and Future Applications of ALD in Micro-Electronics. *ECS Trans.* **2011**, *41* (2), 3–17.

(11) Huang, X. H. X.; Lee, W.-C. L. W.-C.; Kuo, C. K. C.; Hisamoto, D.; Chang, L. C. L.; Kedzierski, J.; Anderson, E.; Takeuchi, H.; Choi, Y.-K. C. Y.-K.; Asano, K.; Subramanian, V.; King, T.-J. K. T.-J.; Bokor, J.; Hu, C. H. C. Sub 50-nm FinFET: PMOS. In *Proceedings of the International Electron Devices Meeting (IEDM)*, Washington, DC, USA; December 5–8, 1999; IEEE, 1999; pp 67–70.

(12) Hu, C.; Lee, W. C.; Kedzierski, J.; Takeuchi, H.; Asano, K.; Kuo, C.; Anderson, E.; King, T. J.; Bokor, J. F.; Hisamoto, D. FinFET-A Self-Aligned Double-Gate MOSFET Scalable to 20 nm. *IEEE Trans. Electron Devices* **2000**, *47* (12), 2320–2325.

(13) Ferain, I.; Colinge, C. A.; Colinge, J.-P. Multigate Transistors as the Future of Classical Metal–oxide–semiconductor Field-Effect Transistors. *Nature* **2011**, *479* (7373), 310–316.

(14) Triyoso, D. H.; Hempel, K.; Ohsiek, S.; Jaschke, V.; Shu, J.; Mutas, S.; Dittmar, K.; Schaeffer, J.; Utess, D.; Lenski, M. Evaluation of Low Temperature Silicon Nitride Spacer for High-k Metal Gate Integration. *ECS J. Solid State Sci. Technol.* **2013**, *2* (11), N222–N227.

(15) Koehler, F.; Triyoso, D. H.; Hussain, I.; Mutas, S.; Bernhardt, H. Atomic Layer Deposition of SiN for Spacer Applications in High-End Logic Devices. *IOP Conf. Ser.: Mater. Sci. Eng.* **2012**, *41*, 012006.

(16) Knoops, H. C. M.; Braeken, E. M. J.; de Peuter, K.; Potts, S. E.; Haukka, S.; Pore, V.; Kessels, W. M. M. Atomic Layer Deposition of Silicon Nitride from Bis(tert-Butylamino)silane and N_2 Plasma. *ACS Appl. Mater. Interfaces* **2015**, *7* (35), 19857–19862.

(17) Robertson, J.; Wallace, R. M. High-k Materials and Metal Gates for CMOS Applications. *Mater. Sci. Eng., R* **2015**, *88*, 1–41.

(18) Boullart, W.; Radisic, D.; Paraschiv, V.; Cornelissen, S.; Manfrini, M.; Yatsuda, K.; Nishimura, E.; Ohishi, T.; Tahara, S. STT MRAM Patterning Challenges. In *Advanced Etch Technology for Nanopatterning II*, Proceedings of SPIE, San Jose, California, USA; February 24, 2013; Zhang, Y., Oehrlein, G. S., Lin, Q., Eds.; SPIE, 2013; p 86850F.

(19) Miyazaki, T.; Tezuka, N. Giant Magnetic Tunneling Effect in $Fe/Al_2O_3/Fe$ Junction. *J. Magn. Magn. Mater.* **1995**, *139* (3), 94–97.

(20) Moodera, J. S.; Kinder, L. R. Ferromagnetic – Insulator – Ferromagnetic Tunneling: Spin-Dependent Tunneling and Large Magnetoresistance in Trilayer Junctions (Invited). *J. Appl. Phys.* **1996**, *79* (8), 4724.

(21) Gaidis, M. C. Magnetoresistive Random Access Memory. In *Nanotechnology*; Wiley-VCH: Weinheim, Germany, 2010; Part 3, Chapter 14, pp 419–446.

(22) Wang, M.; Zhang, Y.; Zhao, X.; Zhao, W. Tunnel Junction with Perpendicular Magnetic Anisotropy: Status and Challenges. *Micromachines* **2015**, *6* (8), 1023–1045.

(23) Gaidis, M. C.; Thomas, L. Magnetic Domain Wall Racetrack Memory. In *Nanoscale Semiconductor Memories*; Kurinec, S. K., Iniewski, K., Eds.; CRC Press: Boca Raton, FL, 2013; pp 229−255.
(24) Liu, X.; Mazumdar, D.; Shen, W.; Schrag, B. D.; Xiao, G. Thermal Stability of Magnetic Tunneling Junctions with MgO Barriers for High Temperature Spintronics. *Appl. Phys. Lett.* **2006**, *89* (2), 21−24.
(25) King, S. W. Plasma Enhanced Atomic Layer Deposition of SiN_x:H and SiO_2. *J. Vac. Sci. Technol., A* **2011**, *29* (4), 41501.
(26) George, S. M. Atomic Layer Deposition: An Overview. *Chem. Rev.* **2010**, *110*, 111.
(27) Profijt, H. B.; Potts, S. E.; van de Sanden, M. C. M.; Kessels, W. M. M. Plasma-Assisted Atomic Layer Deposition: Basics, Opportunities, and Challenges. *J. Vac. Sci. Technol., A* **2011**, *29* (5), 050801.
(28) *Atomic Layer Deposition of Nanostructured Materials*; Pinna, N., Knez, M., Eds.; Wiley-VCH, 2012.
(29) Knoops, H. C. M.; Potts, S. E.; Bol, A. A.; Kessels, W. M. M. Atomic Layer Deposition. In *Handbook of Crystal Growth*; Nishinaga, T., Kuech, T. F., Eds.; Elsevier, 2015; Vol. 3, pp 1101−1134.
(30) Murray, C. A.; Elliott, S. D.; Hausmann, D.; Henri, J.; LaVoie, A. Effect of Reaction Mechanism on Precursor Exposure Time in Atomic Layer Deposition of Silicon Oxide and Silicon Nitride. *ACS Appl. Mater. Interfaces* **2014**, *6*, 10534−10541.
(31) Goto, H.; Shibahara, K.; Yokoyama, S. Atomic Layer Controlled Deposition of Silicon Nitride with Self-Limiting Mechanism. *Appl. Phys. Lett.* **1996**, *68* (23), 3257−3259.
(32) Morishita, S.; Sugahara, S.; Matsumura, M. Atomic-Layer Chemical-Vapor-Deposition of Silicon-Nitride. *Appl. Surf. Sci.* **1997**, *112*, 198−204.
(33) Yokoyama, S.; Ikeda, N.; Kajikawa, K.; Nakashima, Y. Atomic-Layer Selective Deposition of Silicon Nitride on Hydrogen-Terminated Si Surfaces. *Appl. Surf. Sci.* **1998**, *130−132*, 352−356.
(34) Klaus, J. W.; Ott, A. W.; Dillon, A. C.; George, S. M. Atomic Layer Controlled Growth of Si_3N_4 Films Using Sequential Surface Reactions. *Surf. Sci.* **1998**, *418* (1), L14−L19.
(35) Park, K.; Yun, W. D.; Choi, B. J.; Kim, H.; Lee, W. J.; Rha, S. K.; Park, C. O. Growth Studies and Characterization of Silicon Nitride Thin Films Deposited by Alternating Exposures to Si_2Cl_6 and NH_3. *Thin Solid Films* **2009**, *517* (14), 3975−3978.
(36) Riedel, S.; Sundqvist, J.; Gumprecht, T. Low Temperature Deposition of Silicon Nitride Using Si_3Cl_8. *Thin Solid Films* **2015**, *577*, 114−118.
(37) Ovanesyan, R. A.; Hausmann, D. M.; Agarwal, S. Low-Temperature Conformal Atomic Layer Deposition of SiN_x Films Using Si_2Cl_6 and NH_3 Plasma. *ACS Appl. Mater. Interfaces* **2015**, *7* (20), 10806−10813.
(38) Mallikarjunan, A.; Chandra, H.; Xiao, M.; Lei, X.; Pearlstein, R. M.; Bowen, H. R.; O 'neill, M. L.; Derecskei-Kovacs, A.; Han, B. Designing High Performance Precursors for Atomic Layer Deposition of Silicon Oxide. *J. Vac. Sci. Technol., A* **2015**, *33* (1), 01A137.
(39) Park, J.-M.; Jang, S. J.; Yusup, L. L.; Lee, W.-J.; Lee, S.-I. Plasma-Enhanced Atomic Layer Deposition of Silicon Nitride Using a Novel Silylamine Precursor. *ACS Appl. Mater. Interfaces* **2016**, *8* (32), 20865−20871.
(40) Weeks, S.; Nowling, G.; Fuchigami, N.; Bowes, M.; Littau, K.; Weeks, S.; Nowling, G.; Fuchigami, N.; Bowes, M.; Littau, K. Plasma Enhanced Atomic Layer Deposition of Silicon Nitride Using Neopentasilane. *J. Vac. Sci. Technol., A* **2016**, *34* (1), 01A140.
(41) Ande, C. K.; Knoops, H. C. M.; de Peuter, K.; van Drunen, M.; Elliott, S. D.; Kessels, W. M. M. Role of Surface Termination in Atomic Layer Deposition of Silicon Nitride. *J. Phys. Chem. Lett.* **2015**, *6* (18), 3610−3614.
(42) Knoops, H. C. M.; de Peuter, K.; Kessels, W. M. M. Redeposition in Plasma-Assisted Atomic Layer Deposition: Silicon Nitride Film Quality Ruled by the Gas Residence Time. *Appl. Phys. Lett.* **2015**, *107* (1), 014102.
(43) Bosch, R. H. E. C.; Cornelissen, L. E.; Knoops, H. C. M.; Kessels, W. M. M. Atomic Layer Deposition of Silicon Nitride from Bis(Tertiary-Butyl-Amino)Silane and N_2 Plasma Studied by in Situ Gas Phase and Surface Infrared Spectroscopy. *Chem. Mater.* **2016**, *28* (16), 5864−5871.
(44) Xiao, M.; Hochberg, A. K. U.S. Patent No. 7932413. 2011, No. 12.
(45) Thridandam, H.; Xiao, M.; Lei, X.; Gaffney, T. R. U.S. Patent No. 7875312. 2011.
(46) Xiao, M.; Lei, X.; Bowen, H. R.; O'Neill, M. L. U.S. Patent No. 8530361. 2013.
(47) Heil, S. B. S.; van Hemmen, J. L.; Hodson, C. J.; Singh, N.; Klootwijk, J. H.; Roozeboom, F.; van de Sanden, M. C. M.; Kessels, W. M. M. Deposition of TiN and HfO_2 in a Commercial 200 mm Remote Plasma Atomic Layer Deposition Reactor. *J. Vac. Sci. Technol., A* **2007**, *25* (5), 1357.
(48) Knoops, H. C. M.; Langereis, E.; van de Sanden, M. C. M.; Kessels, W. M. M. Conformality of Plasma-Assisted ALD: Physical Processes and Modeling. *J. Electrochem. Soc.* **2010**, *157* (12), G241.
(49) Riley, F. L. Silicon Nitride and Related Materials. *J. Am. Ceram. Soc.* **2000**, *83* (2), 245−265.
(50) Huang, L.; Han, B.; Han, B.; Derecskei-kovacs, A.; Xiao, M.; Lei, X.; O'Neill, M. L.; Pearlstein, R. M.; Chandra, H.; Cheng, H. First-Principles Study of a Full Cycle of Atomic Layer Deposition of SiO_2 Thin Films with Di(sec-Butylamino) Silane and Ozone. *J. Phys. Chem. C* **2013**, *117*, 19454−19463.
(51) Han, B.; Zhang, Q.; Wu, J.; Han, B.; Karwacki, E. J.; Derecskei, A.; Xiao, M.; Lei, X.; O'Neill, M. L.; Cheng, H. On the Mechanisms of SiO_2 Thin-Film Growth by the Full Atomic Layer Deposition Process Using Bis(t-Butylamino)silane on the Hydroxylated SiO_2 (001) Surface. *J. Phys. Chem. C* **2012**, *116* (1), 947−952.
(52) Huang, L.; Han, B.; Han, B.; Derecskei-Kovacs, A.; Xiao, M.; Lei, X.; O'Neill, M. L.; Pearlstein, R. M.; Chandra, H.; Cheng, H. Density Functional Theory Study on the Full ALD Process of Silicon Nitride Thin Film Deposition via BDEAS or BTBAS and NH_3. *Phys. Chem. Chem. Phys.* **2014**, *16* (34), 18501−18512.
(53) Kessels, W. M. M.; van Assche, F. J. H.; Hong, J.; Schram, D. C.; van de Sanden, M. C. M. Plasma Diagnostic Study of Silicon Nitride Film Growth in a Remote $Ar−H_2−N_2−SiH_4$ Plasma: Role of N and SiH_n Radicals. *J. Vac. Sci. Technol., A* **2004**, *22* (1), 96.
(54) Kessels, W. M. M.; van Assche, F. J. H.; van den Oever, P. J.; van de Sanden, M. C. M. The Growth Kinetics of Silicon Nitride Deposited from the $SiH_4−N_2$ Reactant Mixture in a Remote Plasma. *J. Non-Cryst. Solids* **2004**, *338−340*, 37−41.
(55) Hausmann, D.; Henri, J.; Sims, J.; Kelchner, K.; Janjam, S.; Tang, S. *Challenges with Silicon Dielectric Atomic Layer Deposition in High Volume Manufacturing*; Presented at 225th Meeting of the Electrochemical Society: Cancun, Mexico, October 5−9, 2014.
(56) Leick, N.; Ovanesyan, R.; Gasvoda, R.; Walker, P.; Pallem, V.; Lefevre, B.; Kelchner, K.; Hausmann, D.; Agarwal, S. *Surface Reactions during Plasma-Assisted Atomic Layer Deposition of SiN*; Presented at 16th International Conference on Atomic Layer Deposition, Dublin, Ireland, July 24−27, 2016.

DOI: 10.1021/acsami.6b12267
ACS Appl. Mater. Interfaces 2017, 9, 1858−1869